Science Advances

AAAS

advances.sciencemag.org/cgi/content/full/3/7/e1700425/DC1

Supplementary Materials for

Crystal nucleation initiated by transient ion-surface interactions at aerosol interfaces

Ryan D. Davis and Margaret A. Tolbert

Published 19 July 2017, *Sci. Adv.* **3**, e1700425 (2017)
DOI: 10.1126/sciadv.1700425

The PDF file includes:

Other Supplementary Material for this manuscript includes the following:
(available at advances.sciencemag.org/cgi/content/full/3/7/e1700425/DC1)

- movie S1 (.avi format). Near-field tracking of CN-droplet collisions without efflorescence.
- movie S2 (.avi format). Near-field tracking of a CN-droplet collision resulting in efflorescence.
- movie S3 (.avi format). Far-field tracking of CN-droplet collisions without efflorescence.
- movie S4 (.avi format). Far-field tracking of a CN-droplet collision resulting in efflorescence.

- movie S5 (.avi format). Far-field imaging of a droplet with internally mixed PSLs.

Supplementary Text

- **Choice of PSL CN**

Surfactant-free PSLs are commercially available in a wide range of surface functionalities with differing net charges (positive or negative). The ability to vary the surface functionality/charge was necessary in order to probe the ion-specific response to the CN surface. Furthermore, surfactant-free PSLs are used widely and their surface characteristics are thus well characterized. PSLs from the manufacturer (Life Technologies Corp.) have been independently shown via atomic force microscope imaging to have a very low surface roughness (*40*, *41*) and to be clean when aerosolized (*42*). Also, it was essential to use CN that would not significantly absorb the trapping laser wavelength. PSLs have a negligible amount of absorption at 532 nm and were thus suitable for use in our optical trap (*43*). Although PSLs are not found in the atmosphere, the surface functionalities of the PSLs used here (carboxyl and amidine) are similar to insoluble and amorphous organic/carbon-based aerosols found in the atmosphere. Oxidation of aerosol surfaces can lead to carboxyl formation (*35*) and amine-based positive organic ions are observed in marine colloids (*16*) and atmospheric nanoparticles (*44*).

- **Nucleation barrier, collision energy and CN size/composition dependence**

The specific case of NaCl contact efflorescence is discussed here. From classical nucleation theory (CNT) the Gibb's energy barrier to nucleation (ΔG_{nuc}*) for NaCl can be calculated from

$$\Delta G_{nuc}^{*} = \frac{16\pi\gamma^{3}\nu}{3(k_{B}T\ln(S))^{2}} \quad \text{(S1)}$$

where γ is the interfacial tension between the crystal nucleus and the aqueous solution, S is the solute supersaturation, and ν is the molecular volume ($4.48\text{x}10^{-29}$ m^3 for NaCl) (*29*,*30*). At 63±2% RH ($RH_{0.5}^{CE}$ for NaCl contact efflorescence with (−)PSL CN), S = 3.8±0.8, as determined using the E-AIM thermodynamic model (www.aim.env.uea.ac.uk/aim/model3/model3a.php (*26*)). A value for γ is 0.105 N/m for NaCl at 60-70% RH (*29*). Thus, $\Delta G_{nuc}^{*} = 1.3\pm0.5\text{x}10^{-18}$ J (~300 k_BT) at 63% RH. For homogeneous nucleation at ~47% RH (S = 25, γ = 0.0895 N/m) $\Delta G_{nuc}^{*} = 1.4\text{x}10^{-19}$ J (~30 k_BT), an order of magnitude lower than at 63% RH.

The average PSL-droplet collision velocity was 3±1 mm/sec in the experiments reported here. The kinetic energy (KE) of a collision is given by $KE = {}^{1}/_{2}mv^{2}$. For a 400 nm PSL (density = 1.05 g/cm^3, $m = 3.5\text{x}10^{-17}$ kg), KE = $2\pm1\text{x}10^{-22}$ J, which is 3-4 orders of magnitude lower than ΔG_{nuc}*. The average collision velocity was the same for both the 400 nm (+)PSL CN and the 400 nm (−)PSL CN. Thus, KE was the same for both PSL types. There has been evidence to suggest that contact freezing can be promoted when KE of a CN collision with a supercooled water droplet is close to the ice nucleation free energy barrier (*15*). However, this does not appear to be the case in the present study. For all PSL-droplet collisions observed here, KE appears insufficient to influence efflorescence as a result of lowering the free energy barrier to nucleation.

To further test whether a kinetic/mechanical effect may be responsible for our observations, collision-induced NaCl and NH_4Cl contact efflorescence was probed with 800 nm diameter

(−)PSL CN. For an 800 nm PSL, KE = 1.3±0.8x10^{-21} J, which is an order of magnitude higher than with 400 nm diameter PSL CN but still 2-3 orders of magnitude lower than ΔG_{nuc}*. For both NaCl and NH_4Cl, 800 nm (−)PSL CN induced efflorescence at a similar RH as the 400 nm (−)PSL CN, with $RH_{0.5}^{CE}$ values of 66±2 and 51±2% RH for NaCl and NH_4Cl, respectively (see tables S3 and S4 for individual trials), suggesting a nominal CN size dependence. Within this CN size range, CN surface area thus appears to be a minor factor compared to CN surface functionality and aqueous composition, consistent with our previous observations (*7*), further suggesting that crystal nucleation in our studies is related to ion-surface interactions rather than a purely kinetic or mechanical effect.

Further experiments were performed with amorphous sucrose CN and 125 nm diameter surfactant-coated PSL CN. Collisions with amorphous sucrose CN (~0.5-1.5 μm diameter), which were non-ionic and hydrophilic, did not induce efflorescence of aqueous NaCl microdroplets. In contrast, the 125 nm PSL CN were observed to induce efflorescence at an elevated RH relative to homogeneous efflorescence. (However, for PSL CN of this small size, we were unable to confirm that the CN were not aggregates of multiple PSLs. Thus, these experiments were not pursued in detail.) The null-effect of the larger diameter sucrose CN further demonstrate that CN size is not the determining factor and that charge/hydrophobicity are likely the driving forces for our observations.

- **Additional internally-mixed efflorescence experiments**

The null effect of internally-mixed PSLs on the efflorescence RH of NaCl and NH_4Cl was confirmed in two additional ways: by internally mixing PSLs in the trapped droplet at an RH above the deliquescence RH (DRH, above which efflorescence is not be possible) in the same manner that contact efflorescence experiments were performed and then lowering the RH ($\Delta RH/\Delta t \approx 1\%$ RH/min) until efflorescence was observed (5 or more trials); and by deliquescing a crystal that had remained trapped after contact efflorescence and then lowering the RH until the deliquesced droplet effloresced (3 trials). This latter method is the most convincing demonstration of the inactivity of the PSLs once internally mixed as the deliquesced droplet contained the very same PSL that induced efflorescence via a collision, as demonstrated in fig. S4. The former method was performed for all six NaCl and NH_4Cl PSL-droplet combinations (including 800 nm (−)PSLs) while the latter method was successfully performed with NaCl particles that had effloresced upon contact with 400 and 800 nm (−)PSLs. The average efflorescence RH (±1 SD) values in these additional experiments with internally-mixed PSLs were 44±3 and 43±3% RH for NaCl and NH_4Cl, respectively.

- **Estimating the transient effect of (−)PSL collisions on ΔG_{nuc} for NaCl**

According to CNT, the work necessary for the formation of a crystal nucleus with *n* molecules of solute is the change in Gibbs free energy (ΔG_{nuc}) associated with forming the crystal nucleus, which can be expressed as

$$\Delta G_{nuc} = -n\Delta\mu + \Delta G_{surf} \quad \text{(S2)}$$

where ΔG_{surf} is the unfavorable free energy cost of the solid-liquid interface, $\Delta\mu$ is the difference in chemical potential between the metastable aqueous state and the stable crystalline state, and $-n\Delta\mu$ is the favorable decrease in free energy associated with the phase change (*15*,*28-30*). The

$-n\Delta\mu$ term represents the driving force for nucleation and is related to solute supersaturation (S), and thus RH, as $\Delta\mu = k_B T \ln(S)$, where T is temperature and k_B is the Boltzmann constant (*30*). ΔG_{nuc} can be lowered by increasing $\Delta\mu$ or decreasing the contribution of ΔG_{surf}.
Simulations have been performed elsewhere that provide trends in free energy as Na^+ and Cl^- approach a hydrophobic surface and a carboxyl-terminated surface (*22*,*32*), which are relevant to NaCl collision-induced contact efflorescence with (−)PSL CN. These simulations indicate that the free energy of a Na^+ ion increases by ~2-3 $k_B T$ due to compression of its hydration sphere as it forms a solvent-shared ion pair with a charged carboxyl group (*22*). A transient increase in free energy for a single ion would decrease ΔG_{nuc} by that same amount through the $-n\Delta\mu$ term in eq. S2. ΔG_{nuc}* for NaCl at 63% RH is ~300 $k_B T$. A free energy increase of 2 $k_B T$ would thus be sufficient to overcome ΔG_{nuc}* if ~150 Na^+ ions experienced such an increase. The number of ions in a NaCl crystal nucleus, as indicated in simulations, is $n \approx 200$ (*31*), suggesting not all ions in the crystal nucleus would need to experience the transient increase associated with a collision. An increase in interfacial free energy could also serve to lower ΔG_{nuc}* by decreasing ΔG_{surf} (*15*,*28*), leading to the same final effect.

- **Reaching post-collision steady-state water activity**

A functionalized PSL in an aqueous medium is a large solute that will induce changes in water structure in response to the hydrophobic surface as well as the hydrophilic functional groups (*20*,*27*). The addition of a PSL CN to an aqueous droplet via a collision thus introduces a new solute. Prior to a collision, the equilibrium water activity of the droplet will be established by the ions in solution (*26*). Thus, at the moment of contact, there will not be enough water to accommodate and hydrate the PSL CN surface without altering the solvation structure of the ions already present in solution. A non-equilibrium state will exist before additional water vapor can be taken up by the droplet to hydrate the PSL surface. The timescale to achieve a steady-state water concentration is given by $\tau_{SS}=R_d^2/D_v$, where R_d is the droplet radius and D_v is the diffusivity for water vapor (0.282 cm^2/s) (*33*). For a 5 μm radius droplet, $\tau_{SS} \approx 1$ μsec, which is sufficiently long for crystal nucleation to occur (*15*).

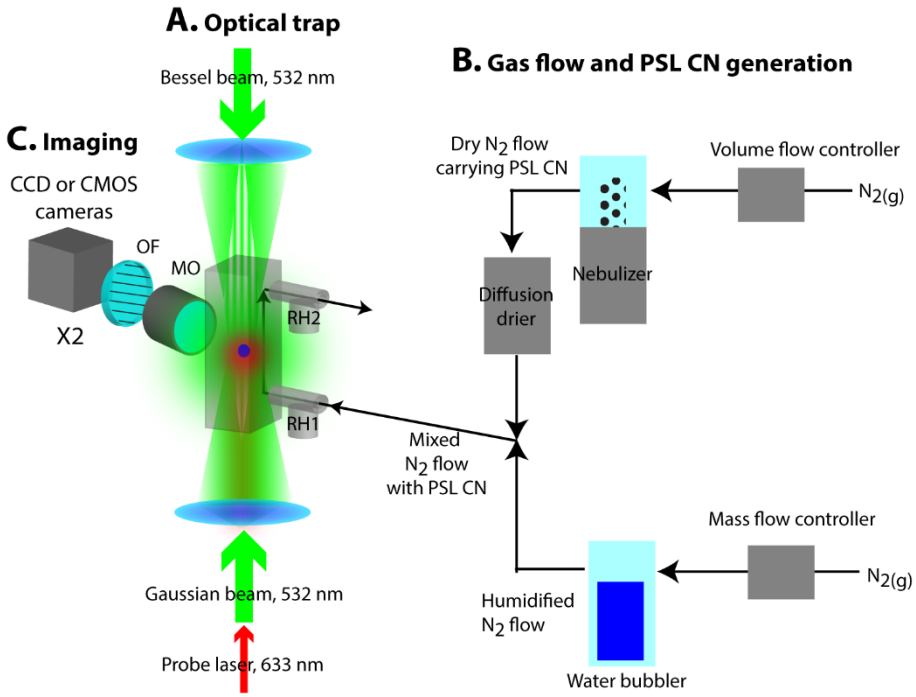

fig. S1. The experimental setup used for efflorescence experiments. (**A**) The optical trapping site is formed from a downward propagating Bessel beam and an upward propagating Gaussian beam. Both trapping beams have a laser wavelength of 532 nm. The levitation chamber is 110 mm long with a circular inner diameter of 12 mm. (**B**) A N_2 gas flow was used to control the RH and to deliver the PSL CN into the levitation chamber. PSL CN were wet generated with a medical nebulizer and dried in a diffusion drier. The dry N_2 gas flow carrying the PSL CN was mixed with a N_2 gas flow that was humidified with a water bubbler prior to entering the levitation chamber through a bottom port. RH probes were placed before and after the flow tube (RH1 and RH2). The RH at the center of the levitation chamber was taken as the mean of RH1 and RH2 (±1 SD). (**C**) Elastically scattered 532 nm laser light was collected with a microscope objective (MO) and an optical polarization filter (OF) and imaged in the far-field using a CCD camera. Near-field scattered laser light from a 632.8 nm HeNe probe laser was collected with an MO and an optical band-pass filter (OF) and imaged with a CMOS camera.

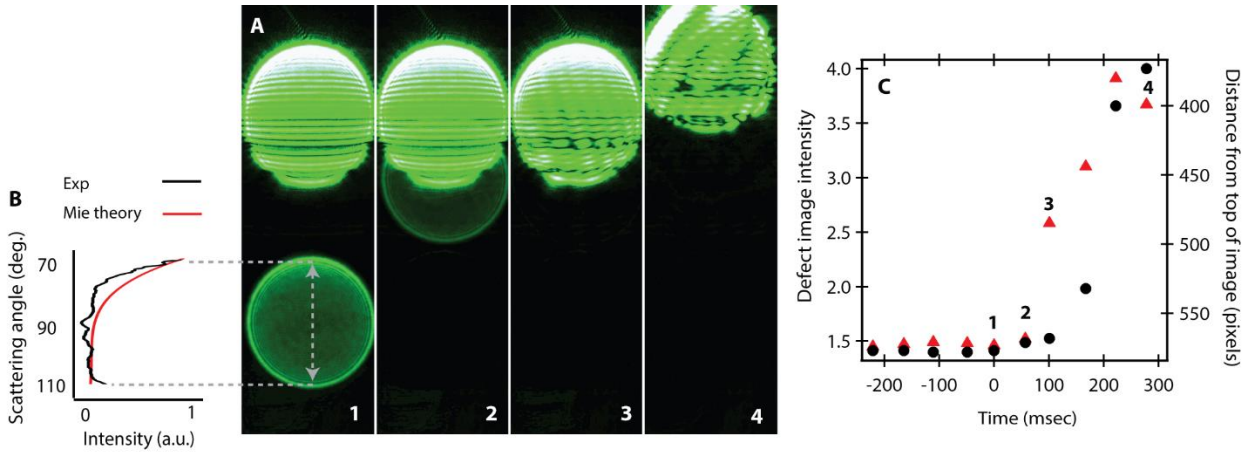

fig. S2. Image processing to detect collisions and efflorescence. (**A**) A sequence of images of far-field elastically scattered laser light (532 nm wavelength) capturing a 400 nm (−)PSL contacting an NaCl droplet and inducing efflorescence at RH=58±1% RH. In frame 1 (t = 0 msec), the droplet is at the top of the image and the PSL CN is seen at the bottom of the image. The horizontal linear interference fringes are indicative of a spherical and liquid droplet. In frame 2 (t = 57 msec), the PSL CN has moved closer to the droplet. In frame 3 (t = 101 msec) contact and the onset of crystal growth are apparent by the breakdown in the linear interference fringes. In frame 4 (t = 278 msec), crystal growth has progressed, as evident by the further breakdown in the interference fringes and the upwards movement associated with loss of water mass due to efflorescence. (**B**) Mie theory calculation compared to the experimental phase function of the 400 nm PSL in frame 1 of part A, which was determined by measuring the intensity of scattered laser light collected by the microscope objective, demonstrating that the PSL CN is a single particle and not an aggregate of multiple PSLs. (**C**) The image analysis data used to detect efflorescence of the droplet. The defect image intensity (red triangles) quantifies the breakdown in the interference fringes (see Materials and Methods) while the position of the droplet (black circles) indicates loss of water mass due to efflorescence. The numbers on the plot (1-4) correspond to the values determined for frames 1-4 of part A.

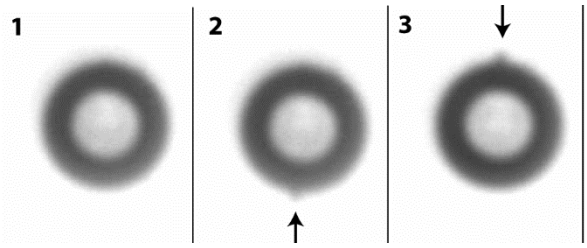

fig. S3. Bright-field images of a droplet with internally mixed PSLs. A sequence of bright-field images of contact and subsequent internal mixing (without efflorescence) of an 800 nm (−)PSL with a NH_4Cl droplet at 55±2% RH. Frame 1 shows the droplet before contact. Frame 2 shows the droplet after contact. The PSL, is evident at the bottom of the droplet where indicated by the arrow. In frame 3, the PSL has gradually moved to the top of the droplet over a period of ~1.5 sec and remains at the droplet surface.

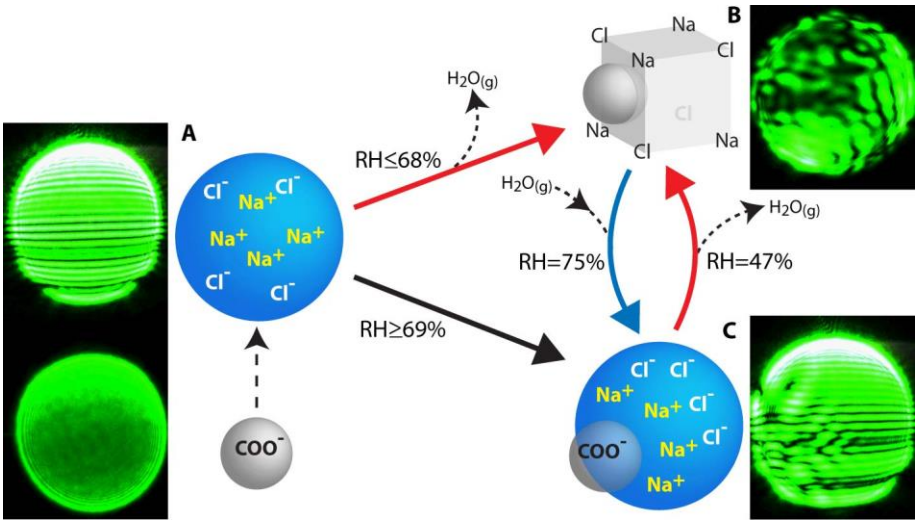

fig. S4. Contact efflorescence–deliquescence–internally mixed efflorescence cycle. Contact efflorescence (A to B) − deliquescence (B to C) − internally-mixed efflorescence (C to B) cycle of a NaCl particle that effloresced upon contact. Illustrations depict what is shown in the far-field images of scattered laser light (outer inset images). (**A**) Optically levitated NaCl microdroplet (~10 µm diameter) prior to a collision with an 800 nm (−) PSL CN. (**B**) Effloresced crystal with PSL internally mixed. (**C**) Aqueous droplet with internally-mixed PSL evident at the droplet surface. Efflorescence (red arrows) occurred at remarkably different RH values, depending on whether the PSL made external contact (A to B) or was internally mixed in the droplet (C to B). (**A-B**) NaCl collision-induced contact efflorescence was observed as high as 68±1% RH. (**B-C**) Deliquescence of the effloresced crystal (blue arrow) resulted in an aqueous droplet with the PSL internally mixed. (**C-B**) Upon decreasing RH, internally-mixed efflorescence was not observed until ~44±3% RH, consistent with homogeneous efflorescence, demonstrating that PSL CN had no influence on crystal nucleation except at the moment of contact, regardless of how a PSL became internally mixed with a droplet (i.e., A to C or B to C). Rearrangement of ions and water molecules at the PSL-droplet interface is expected upon contact (demonstrated in A to C).

table S1. Manufacturer-stated properties of the PSL CN.

PSL type	Lot #	Mean diameter ±1 SD (nm)	Surface charge group	Maximum surface charge density ($\mu C/cm^2$)	Surface area per charge group ($Å^2$)
(+)PSL, 400 nm	1169658	400±13	Amidine ($NH_2NH_2^+/NH_2NH$)	19.2	84
(−)PSL, 400 nm	1613903	400±12	Carboxyl ($COO^-/COOH$)	−7.3	218
(−)PSL, 800 nm	1769589	780±21	Carboxyl ($COO^-/COOH$)	−7.6	211

table S2. Homogeneous and internally mixed efflorescence results.

Droplet	Experiment type (H = homogeneous, IM = internally-mixed PSLs)	N_{tot}	N_{eff}	RH bin median (%) ± upper /lower quartile	$P_{hom} \pm N_{tot}^{-1/2}$	$P_{IM} \pm N_{tot}^{-1/2}$
NaCl	H	12	12	46±1	1.0±0.3	--
NaCl	H	14	6	47±1	0.4±0.3	--
NaCl	H	14	0	48±1	0.0±0.3	--
NaCl	H	14	0	49±1	0.0±0.3	--
NaCl	IM, (−)PSL, 400 nm dia.	15	15	46±1	--	1.0±0.3
NaCl	IM, (−)PSL, 400 nm dia.	15	8	47±1	--	0.5±0.3
NaCl	IM, (−)PSL, 400 nm dia.	15	0	48±1	--	0.0±0.3
NaCl	IM, (−)PSL, 400 nm dia.	15	0	49±1	--	0.0±0.3
NaCl	IM, (+)PSL, 400 nm dia.	15	15	46±1	--	1.0±0.3
NaCl	IM, (+)PSL, 400 nm dia.	15	7	47±1	--	0.5±0.3
NaCl	IM, (+)PSL, 400 nm dia.	15	0	48±1	--	0.0±0.3
NaCl	IM, (+)PSL, 400 nm dia.	15	0	50±1	--	0.0±0.3
NaCl	IM total (reported in Fig. 1)	30	30	46±1	--	1.0±0.2
NaCl	IM total (reported in Fig. 1)	30	15	47±1	--	0.5±0.2
NaCl	IM total (reported in Fig. 1)	30	0	48±1	--	0.0±0.2
NaCl	IM total	30	0	49±1	--	0.0±0.2
NH_4Cl	H	12	12	44±1	1.0±0.3	--
NH_4Cl	H	12	5	45±1	0.4±0.3	--
NH_4Cl	H	10	0	46±1	0.0±0.3	--
NH_4Cl	H	10	0	49±1	0.0±0.3	--
NH_4Cl	IM, (−)PSL, 400 nm dia.	10	10	44±1	--	1.0±0.3
NH_4Cl	IM, (−)PSL, 400 nm dia.	10	5	45±1	--	0.5±0.3
NH_4Cl	IM, (−)PSL, 400 nm dia.	10	0	46±1	--	0.0±0.3
NH_4Cl	IM, (−)PSL, 400 nm dia.	10	0	48±1	--	0.0±0.3
NH_4Cl	IM, (+)PSL, 400 nm dia.	10	10	44±1	--	1.0±0.3
NH_4Cl	IM, (+)PSL, 400 nm dia.	10	4	45±1	--	0.4±0.3
NH_4Cl	IM, (+)PSL, 400 nm dia.	10	0	46±1	--	0.0±0.3
NH_4Cl	IM, (+)PSL, 400 nm dia.	10	0	49±1	--	0.0±0.3
NH_4Cl	IM total (reported in Fig. 1)	20	20	44±1	--	1.0±0.2
NH_4Cl	IM total (reported in Fig. 1)	20	9	45±1	--	0.5±0.2
NH_4Cl	IM total (reported in Fig. 1)	20	0	46±1	--	0.0±0.2
NH_4Cl	IM total	20	0	49±2	--	0.0±0.2
NaBr	H	15	15	25±2	1.0±0.3	--
NaBr	H	15	9	26±2	0.6±0.3	--
NaBr	H	15	0	27±2	0.0±0.3	--
NaBr	H	15	0	29±2	0.0±0.3	--
NaBr	IM, (−)PSL, 400 nm dia.	15	15	25±1	--	1.0±0.3
NaBr	IM, (−)PSL, 400 nm dia.	15	8	26±1	--	0.5±0.3
NaBr	IM, (−)PSL, 400 nm dia.	15	3	28±1	--	0.2±0.3
NaBr	IM, (−)PSL, 400 nm dia.	15	5	31±1	--	0.3±0.3
NaBr	IM, (−)PSL, 400 nm dia.	15	4	36±1	--	0.3±0.3
NaBr	IM, (−)PSL, 400 nm dia.	15	0	40±1	--	0.0±0.3
NaBr	IM, (+)PSL, 400 nm dia.	15	15	25±1	--	1.0±0.3
NaBr	IM, (+)PSL, 400 nm dia.	15	8	26±1	--	0.5±0.3

NaBr	IM, (+)PSL, 400 nm dia.	32	6	28±2	--	0.2±0.2
NaBr	IM, (+)PSL, 400 nm dia.	15	3	30±1	--	0.2±0.3
NaBr	IM, (+)PSL, 400 nm dia.	15	3	36±1	--	0.2±0.3
NaBr	IM, (+)PSL, 400 nm dia.	15	0	40±1	--	0.0±0.3
NaBr	IM total (reported in Fig. 1)	30	30	25±1	--	1.0±0.2
NaBr	IM total (reported in Fig. 1)	30	16	26±1	--	0.5±0.2
NaBr	IM total (reported in Fig. 1)	47	9	28±2	--	0.2±0.1
NaBr	IM total (reported in Fig. 1)	30	8	31±1	--	0.3±0.2
NaBr	IM total (reported in Fig. 1)	30	7	36±1	--	0.2±0.2
NaBr	IM total (reported in Fig. 1)	30	0	40±1	--	0.0±0.2

table S3. NaCl contact efflorescence results for individual trials.

PSL CN type	RH (%)	RH error (±1 SD)	Collisions	Outcome (1 = effloresced, 0 = remained liquid)	**RH bin median (%) ± lower /upper quartile**	$P_{CE} \pm N_{col}^{-1/2}$
(−)PSL, 400 nm	52.1	1.1	1	1		
(−)PSL, 400 nm	52.3	2.2	1	1		
(−)PSL, 400 nm	52.5	2.0	3	1		
(−)PSL, 400 nm	52.6	3.1	1	1		
(−)PSL, 400 nm	52.7	2.5	1	1		
(−)PSL, 400 nm	53	3.0	1	1		
			N_{col} = 8	**N_{eff} = 6**	**53±3**	**0.8±0.3**
(−)PSL, 400 nm	56.9	0.7	1	1		
(−)PSL, 400 nm	56.9	0.7	1	1		
(−)PSL, 400 nm	57.2	1.3	1	1		
(−)PSL, 400 nm	57.3	0.9	1	1		
(−)PSL, 400 nm	57.7	1.1	1	1		
			N_{col} = 5	**N_{eff} = 5**	**57±1**	**1.0±0.4**
(−)PSL, 400 nm	61.1	2.0	1	1		
(−)PSL, 400 nm	61.7	0.9	1	1		
(−)PSL, 400 nm	61.9	0.7	1	1		
(−)PSL, 400 nm	62.1	1.8	1	1		
(−)PSL, 400 nm	62.1	0.8	1	1		
			N_{col} = 5	**N_{eff} = 5**	**62±1**	**1.0±0.4**
(−)PSL, 400 nm	63.1	1.8	2	1		
(−)PSL, 400 nm	63.2	1.2	4	1		
(−)PSL, 400 nm	63.6	0.5	9	1		
(−)PSL, 400 nm	63.7	0.7	8	1		
(−)PSL, 400 nm	63.8	0.5	2	1		
			N_{col} = 25	**N_{eff} = 5**	**64±1**	**0.2±0.2**
(−)PSL, 400 nm	64.9	0.8	8	1		
(−)PSL, 400 nm	65.1	1.0	10	0		
(−)PSL, 400 nm	65.3	0.8	5	1		
(−)PSL, 400 nm	65.4	1.4	10	0		
(−)PSL, 400 nm	65.5	0.8	5	1		
(−)PSL, 400 nm	65.6	0.5	6	1		
(−)PSL, 400 nm	65.9	0.5	8	0		
(−)PSL, 400 nm	65.9	0.5	9	0		
			N_{col} = 61	**N_{eff} = 4**	**66±1**	**0.1±0.1**
(−)PSL, 800 nm	48.6	3.0	1	1		
(−)PSL, 800 nm	48.9	3.0	1	1		
(−)PSL, 800 nm	50.8	2.9	1	1		
(−)PSL, 800 nm	51.1	2.6	1	1		
			N_{col} = 4	**N_{eff} = 4**	**50±4**	**1.0±0.5**
(−)PSL, 800 nm	52	3.0	1	1		
(−)PSL, 800 nm	52.9	2.8	1	1		
(−)PSL, 800 nm	53.6	3.0	1	1		
(−)PSL, 800 nm	54.1	3.0	1	1		

(−)PSL, 800 nm	54.3	2.7	1	1		
			N_{col} = 5	**N_{eff} = 5**	**54±3**	**1.0±0.4**
(−)PSL, 800 nm	55.0	3.1	1	1		
(−)PSL, 800 nm	55.5	3.0	1	1		
(−)PSL, 800 nm	56.7	2.2	1	1		
(−)PSL, 800 nm	56.8	1.7	1	1		
			N_{col} = 4	**N_{eff} = 4**	**56±2**	**1.0±0.5**
(−)PSL, 800 nm	63.7	1.0	1	1		
(−)PSL, 800 nm	63.8	0.9	1	1		
(−)PSL, 800 nm	63.8	0.7	1	1		
(−)PSL, 800 nm	64.0	0.5	1	1		
(−)PSL, 800 nm	64.2	0.5	1	1		
			N_{col} = 5	**N_{eff} = 5**	**64±1**	**1.0±0.4**
(−)PSL, 800 nm	66.6	0.5	4	1		
(−)PSL, 800 nm	66.7	1.0	5	1		
(−)PSL, 800 nm	66.7	0.8	6	1		
(−)PSL, 800 nm	66.9	1.2	2	1		
			N_{col} = 17	**N_{eff} = 4**	**67±1**	**0.2±0.2**
(−)PSL, 800 nm	68.4	0.7	7	0		
(−)PSL, 800 nm	68.4	0.7	3	1		
(−)PSL, 800 nm	68.5	1.2	7	0		
(−)PSL, 800 nm	69.0	1.0	8	0		
			N_{col} = 25	**N_{eff} = 1**	**69±1**	**0.0±0.2**
(+)PSL, 400 nm	49.5	1.5	1	1		
(+)PSL, 400 nm	49.5	1.3	1	1		
(+)PSL, 400 nm	51.6	1.8	2	1		
(+)PSL, 400 nm	51.7	1.3	1	1		
(+)PSL, 400 nm	51.9	1.9	1	1		
(+)PSL, 400 nm	52.1	2.0	1	1		
			N_{col} = 7	**N_{eff} = 6**	**52±2**	**0.9±0.4**
(+)PSL, 400 nm	55.1	1.5	1	1		
(+)PSL, 400 nm	55.6	1.3	2	1		
(+)PSL, 400 nm	56.0	1.5	2	1		
(+)PSL, 400 nm	56.4	1.5	1	1		
			N_{col} = 6	**N_{eff} = 4**	**56±2**	**0.7±0.4**
(+)PSL, 400 nm	56.8	1.5	3	1		
(+)PSL, 400 nm	57.6	1.4	7	0		
(+)PSL, 400 nm	57.6	1.6	10	0		
(+)PSL, 400 nm	57.6	1.5	8	1		
(+)PSL, 400 nm	57.7	1.5	7	1		
			N_{col} = 35	**N_{eff} = 3**	**58±2**	**0.1±0.2**

table S4. NH_4Cl contact efflorescence results for individual trials.

PSL CN type	RH (%)	RH error (±1 SD)	Collisions	Outcome (1 = effloresced, 0 = remained liquid)	**RH bin median (%) ± upper /lower quartile**	$P_{CE} \pm N_{col}^{-1/2}$
(−)PSL, 400 nm	46.2	1.2	1	1		
(−)PSL, 400 nm	47.8	1.2	1	1		
(−)PSL, 400 nm	47.8	0.8	1	1		
(−)PSL, 400 nm	47.8	0.5	1	1		
(−)PSL, 400 nm	48.0	0.5	1	1		
			N_{col} = 5	**N_{eff} = 5**	**48±1**	**1.0±0.4**
(−)PSL, 400 nm	49.6	1.3	4	1		
(−)PSL, 400 nm	50.3	0.9	2	1		
(−)PSL, 400 nm	50.4	1.4	1	1		
(−)PSL, 400 nm	50.4	0.5	2	1		
(−)PSL, 400 nm	50.4	0.8	3	1		
			N_{col} = 12	**N_{eff} = 5**	**50±1**	**0.4±0.3**
(−)PSL, 400 nm	52.1	0.5	10	0		
(−)PSL, 400 nm	51.7	0.5	10	0		
(−)PSL, 400 nm	51.5	0.9	10	0		
(−)PSL, 400 nm	51.7	1.1	10	0		
			N_{col} = 40	**N_{eff} = 0**	**52±1**	**0.0±0.2**
(−)PSL, 400 nm	54.1	0.6	10	0		
(−)PSL, 400 nm	54.2	0.5	10	0		
(−)PSL, 400 nm	54.2	0.5	10	0		
(−)PSL, 400 nm	54.3	0.5	10	0		
			N_{col} = 40	**N_{eff} = 0**	**54±1**	**0.0±0.2**
(−)PSL, 800 nm	50	0.5	1	1		
(−)PSL, 800 nm	50.2	0.5	1	1		
(−)PSL, 800 nm	50.2	0.6	1	1		
(−)PSL, 800 nm	50.2	0.5	1	1		
(−)PSL, 800 nm	50.2	0.5	1	1		
			N_{col} = 5	**N_{eff} = 5**	**50±1**	**1.0 ±0.4**
(−)PSL, 800 nm	51.5	0.5	3	1		
(−)PSL, 800 nm	51.5	1	2	1		
(−)PSL, 800 nm	51.6	0.5	2	1		
(−)PSL, 800 nm	51.9	0.5	1	1		
(−)PSL, 800 nm	52.1	0.5	6	0		
(−)PSL, 800 nm	52.3	0.5	7	0		
(−)PSL, 800 nm	52.5	0.7	5	0		
			N_{col} = 26	**N_{eff} = 4**	**52±1**	**0.2±0.2**
(−)PSL, 800 nm	54.3	1.8	10	0		
(−)PSL, 800 nm	54.3	1.5	10	0		
(−)PSL, 800 nm	54.3	1.3	7	0		
(−)PSL, 800 nm	54.6	1.3	6	0		
			N_{col} = 33	**N_{eff} = 0**	**54±2**	**0.0±0.2**
(+)PSL, 400 nm	53.5	0.5	1	1		
(+)PSL, 400 nm	53.5	0.5	1	1		

(+)PSL, 400 nm	53.5	0.5	1	1		
(+)PSL, 400 nm	53.9	0.5	1	1		
(+)PSL, 400 nm	54.7	0.5	1	1		
(+)PSL, 400 nm	55.1	2	2	1		
			N_{col} = 7	**N_{eff} = 6**	**54±1**	**1.0±0.4**
(+)PSL, 400 nm	56.9	2.2	1	1		
(+)PSL, 400 nm	57.2	1.3	2	1		
(+)PSL, 400 nm	57.4	1.4	2	1		
(+)PSL, 400 nm	57.7	0.7	1	1		
(+)PSL, 400 nm	58.6	1.9	2	1		
(+)PSL, 400 nm	58.6	1.9	1	1		
			N_{col} = 9	**N_{eff} = 6**	**58±2**	**0.7±0.3**
(+)PSL, 400 nm	60.2	0.5	4	1		
(+)PSL, 400 nm	60.2	0.5	3	1		
(+)PSL, 400 nm	60.3	0.5	2	1		
(+)PSL, 400 nm	60.4	0.8	1	1		
(+)PSL, 400 nm	60.8	0.5	5	1		
			N_{col} = 15	**N_{eff} = 5**	**60±1**	**0.3±0.3**
(+)PSL, 400 nm	62.3	0.6	10	0		
(+)PSL, 400 nm	62.4	0.5	10	0		
(+)PSL, 400 nm	62.4	0.6	10	0		
(+)PSL, 400 nm	62.9	2.8	10	0		
			N_{col} = 40	**N_{eff} = 0**	**62±1**	**0.0±0.2**

table S5. NaBr contact efflorescence results for individual trials.

PSL CN type	RH (%)	RH error (±1 SD)	Collisions	Outcome (1 = effloresced, 0 = remained liquid)	**RH bin median (%) ± upper /lower quartile**	$P_{CE} \pm N_{col}^{-1/2}$
(−)PSL, 400 nm	28.8	2	1	1		
(−)PSL, 400 nm	28.6	2	1	1		
(−)PSL, 400 nm	28.1	2	1	1		
(−)PSL, 400 nm	27.7	1.9	1	1		
(−)PSL, 400 nm	27.7	1.9	1	1		
			N_{col} = 5	**N_{eff} = 5**	**28±2**	**1.0±0.4**
(−)PSL, 400 nm	35	3.6	1	1		
(−)PSL, 400 nm	35.8	2.5	1	1		
(−)PSL, 400 nm	37.4	1.8	1	1		
(−)PSL, 400 nm	37.8	2.1	1	1		
(−)PSL, 400 nm	37.6	1.9	1	1		
			N_{col} = 12	**N_{eff} = 5**	**37±2**	**1.0±0.4**
(−)PSL, 400 nm	39.9	0.7	1	1		
(−)PSL, 400 nm	39.1	0.7	1	1		
(−)PSL, 400 nm	39.5	0.9	1	1		
(−)PSL, 400 nm	39.6	1	1	1		
(−)PSL, 400 nm	40.1	0.5	1	1		
(−)PSL, 400 nm	40.7	1.4	1	1		
(−)PSL, 400 nm	40.1	0.5	1	1		
			N_{col} = 7	**N_{eff} = 7**	**40±1**	**1.0±0.4**
(−)PSL, 400 nm	41.2	0.6	1	1		
(−)PSL, 400 nm	41.7	0.5	5	0		
(−)PSL, 400 nm	41.9	0.5	4	0		
(−)PSL, 400 nm	41.6	1.3	6	0		
(−)PSL, 400 nm	41.6	1.2	1	1		
(−)PSL, 400 nm	41.3	1.2	6	0		
(−)PSL, 400 nm	41.6	1.2	1	1		
(−)PSL, 400 nm	41.2	1.2	1	1		
			N_{col} = 25	**N_{eff} = 4**	**42±1**	**0.2±0.2**
(−)PSL, 400 nm	43.4	0.5	5	0		
(−)PSL, 400 nm	43.9	0.5	6	0		
(−)PSL, 400 nm	44.1	0.5	9	0		
(−)PSL, 400 nm	43.8	1.4	10	0		
(−)PSL, 400 nm	44.2	0.5	6	0		
			N_{col} = 36	**N_{eff} = 0**	**44±1**	**0.0±0.2**
(+)PSL, 400 nm	29.8	2.3	2	1		
(+)PSL, 400 nm	29.8	2.2	1	1		
(+)PSL, 400 nm	29.8	2.2	1	1		
(+)PSL, 400 nm	29.6	1.6	2	1		
(+)PSL, 400 nm	28.4	0.8	1	1		
(+)PSL, 400 nm	28.4	0.8	2	1		
(+)PSL, 400 nm	28.8	1.3	2	1		
(+)PSL, 400 nm	28.8	1.3	2	1		

(+)PSL, 400 nm	27.9	0.5	3	1		
(+)PSL, 400 nm	27.4	2.9	2	1		
(+)PSL, 400 nm	26.5	2.4	4	1		
(+)PSL, 400 nm	26.4	0.8	2	1		
(+)PSL, 400 nm	26.6	0.8	1	1		
(+)PSL, 400 nm	26.8	1.3	3	1		
			N_{col} = 28	**N_{eff} = 14**	**28±2**	**0.5±0.2**
(+)PSL, 400 nm	32	2.7	4	1		
(+)PSL, 400 nm	32	0.5	4	1		
(+)PSL, 400 nm	32.5	0.9	3	1		
(+)PSL, 400 nm	32.5	0.9	1	1		
(+)PSL, 400 nm	32.6	1.1	3	1		
(+)PSL, 400 nm	32.6	1.1	3	1		
			N_{col} = 18	**N_{eff} = 6**	**33±1**	**0.3±0.2**
(+)PSL, 400 nm	38	3.4	7	1		
(+)PSL, 400 nm	37.7	0.5	1	1		
(+)PSL, 400 nm	37.1	0.5	1	1		
(+)PSL, 400 nm	37.4	1.1	4	1		
(+)PSL, 400 nm	37.5	2.1	7	1		
(+)PSL, 400 nm	39	0.5	2	1		
(+)PSL, 400 nm	39	0.5	6	1		
(+)PSL, 400 nm	39	0.6	8	1		
(+)PSL, 400 nm	39.5	1.1	6	0		
			N_{col} = 42	**N_{eff} = 8**	**38±2**	**0.2±0.2**
(+)PSL, 400 nm	40.4	0.5	9	0		
(+)PSL, 400 nm	40.8	0.9	6	0		
(+)PSL, 400 nm	40.8	0.9	8	0		
(+)PSL, 400 nm	41.1	1.1	5	0		
(+)PSL, 400 nm	41.3	1.1	8	0		
			N_{col} = 36	**N_{eff} = 0**	**41±1**	**0.0±0.2**

Movie Captions

movie S1. Near-field tracking of CN-droplet collisions without efflorescence. An example of using near-field imaging of laser scatter from the 632.8 nm HeNe probe laser to track CN-droplet collisions that did not induce efflorescence. The droplet was aqueous NH_4Cl at 54±2% RH and the PSL CN were 800 nm (−)PSLs. Images were captured in monochrome at ~140 fps with playback here at 20 fps (~7X slower than real time). The droplet is positioned in the middle of the frame. Initially, no PSL CN are visible. After ~4 sec, a PSL CN can be seen entering the image from the bottom of the frame and then make contact with the droplet. In this example, efflorescence does not occur. The presence of the PSL is evident at the droplet surface on the right side of the droplet shortly after contact, particularly at ~8 sec. At ~12 sec, another PSL CN enters the frame and passes the droplet (does not make contact).

movie S2. Near-field tracking of a CN-droplet collision resulting in efflorescence. An example of using near-field imaging of laser scatter from the 632.8 nm HeNe probe laser to track a CN-droplet collision for NH_4Cl contact efflorescence at 50±1% RH. The PSL CN was an 800 nm (−)PSL. Images were captured in monochrome at ~140 fps with playback here at 20 fps (~7X slower than real time). Initially, no PSL CN are visible. At ~2 sec, two PSL CN enter the frame. One does not make contact whereas the other makes contact and induces efflorescence immediately. Efflorescence is evident by the change in laser scatter pattern and the abrupt upward movement due to loss of water mass.

movie S3. Far-field tracking of CN-droplet collisions without efflorescence. An example of using far-field imaging of laser scatter from the 532 nm trapping lasers to track a CN-droplet collision that did not induce efflorescence. The droplet was aqueous NaCl at 69±1% RH and the PSL CN was an 800 nm (−)PSL. Images were captured at ~20 fps with playback here at 20 fps (ca. real time). The droplet is positioned at the top of the frame. Initially, no PSL CN are visible. Note that at the start of the movie, the horizontal linear interference fringes are uniform. After ~2 sec, a PSL CN can be seen entering the image from the bottom of the frame and then make contact with the droplet. In this example, efflorescence does not occur. The presence of the PSL is evident at the droplet surface by the disruption in the linear interference fringes. The PSL remains at or near the droplet surface after the collision.

movie S4. Far-field tracking of a CN-droplet collision resulting in efflorescence. An example of using far-field imaging of laser scatter from the 532 nm trapping lasers to track a CN-droplet collision for NaCl contact efflorescence at 57±2% RH. The PSL CN was an 800 nm (−)PSL. Images were captured at ~20 fps with playback here at 20 fps (ca. real time). Initially, no PSL CN are visible. Note that at the start of the movie, the horizontal linear interference fringes are uniform. After ~2 sec, a PSL CN can be seen entering the image from the bottom of the frame and then make contact with the droplet. Efflorescence is initiated immediately, as evident not only by the disruption in the linear interference fringes but also by the upward movement of the levitated particle due to loss of water mass. The efflorescing particle is momentarily removed from the field-of-view of the camera and briefly lost from the trap. Once the fully effloresced particle re-establishes an equilibrium position in the trap, it is clear from the irregular laser scatter that the particle is crystalline, as can be seen at the top of the frame at ~5 sec.

movie S5. Far-field imaging of a droplet with internally mixed PSLs. An example of the far-field 532 nm laser scatter for a NaCl droplet with pre-internally-mixed 400 nm (−)PSLs at 48±1% RH. The presence of the PSLs is evident by the disruption in the linear interference fringes that are typical of a pure droplet. Comparison of these images to those shown post-collision in movie S3 demonstrate that the interference pattern is similar in both cases, suggesting that the location of the PSLs in the droplet was the same regardless of whether the PSLs were pre-internally-mixed or became internally mixed after a collision.